Acta et Commentationes, Exact and Natural Sciences
Volume 19(1), 2025, Pages 28–42
CZU: 547.022.1/.4:579.84/.86
ISSN: 2537-6284
E-ISSN: 2587-3644
DOI: 10.36120/2587-3644.v19i1.28-42

Synthesis, characterization, structural analysis and antimicrobial activity of bis(*m*-phenylenediamine)tetraoxime

Dumitru Ureche, Ion Bulhac, Alexandru Ciocarlan, Lucian Lupascu, and Pavlina Bourosh

Abstract. The synthesis of a new tetraoxime, $H_4L{\cdot}2DMF$ (**1**), was achieved in 60% yield by the reaction of dichloroglyoxime ($DClH_2$) with *m*-phenylenediamine in a 1:1 molar ratio in ethanol and DMF. Its structure was confirmed by FTIR spectroscopy, as well as by ^1H, ^{13}C, and ^{15}N NMR analyses, and single-crystal X-ray diffraction. In addition, the antimicrobial activity of this compound was investigated. Under similar conditions and in the presence of Zn(II) ions, a new polymorph of compound **1** – $H_4L{\cdot}2DMF$ (**2**) – was obtained, and in the presence of Mn(II) or Gd(III) ions, two new solvatomorphs $H_4L{\cdot}3.5H_2O$ (**3**) and $H_4L{\cdot}2C_2H_5OH{\cdot}0.33H_2O$ (**4**), were synthesized. Their structures were confirmed by single-crystal X-ray analysis.

Keywords: tetraoxime, *m*-phenylenediamine, antimicrobial activity, X-ray diffraction, NMR and IR spectroscopy.

Sinteza, caracterizarea, analiza structurală și activitatea antimicrobiană a bis(*m*-fenilendiamin)tetraoximei

Rezumat. Sinteza unei noi tetraoxime, $H_4L{\cdot}2DMF$ (**1**), a fost realizată cu un randament de 60% prin reacția dintre dicloroglioximă ($DClH_2$) și *m*-fenilendiamină într-un raport molar de 1:1, în etanol și DMF. Structura sa a fost confirmată prin spectroscopie FTIR, analize NMR de ^1H, ^{13}C, ^{15}N, precum și prin difracție razelor X pe monocristal. În plus, a fost investigată activitatea antimicrobiană a acestui compus. În condiții similare și în prezența ionilor de Zn(II), a fost obținut un nou polimorf al compusului 1 – $H_4L{\cdot}2DMF$ (**2**). De asemenea, în prezența ionilor de Mn(II) sau Gd(III), au fost sintetizați doi solvatomorfi noi, $H_4L{\cdot}3.5H_2O$ (**3**) și $H_4L{\cdot}2C_2H_5OH{\cdot}0.33H_2O$ (**4**). Structurile acestora au fost confirmate prin analiza difracției razelor X pe monocristal.

Cuvinte-cheie: tetraoximă, *m*-fenilendiamină, activitate antimicrobiană, difracția razelor X, spectroscopie RMN și IR.

1. Introduction

The most common *vic*-dioximes are used as general industrial chemicals [1], while oxime ligands are used as analytical reagents or as models for natural biological systems

and as catalysts in various chemical processes [2, 3, 4]. They have attracted considerable attention as model compounds for the study of some biofunctions in natural systems, including the reduction of vitamin B_{12} [5]. Most of the dioximes also exhibit a wide range of pharmacological properties, such as antibacterial, antidepressant, and antifungal activities [6, 7, 8]. Oximes and their metal complexes are of great interest due to the diversity of their physicochemical properties, including their role as reactivity models and potential applications in many important chemical processes in medicine [9, 10, 11, 12], bioorganic systems [13, 14], and catalysis [15], as well as in electrochemical [16] and electro-optical sensors [17, 18].

Macrocyclic *vic*-dioximes, such as those of the tetraoxime type, can be obtained by the interaction of diamines or thiols with dichloroglyoxime ($DClH_2$) [2, 19, 20]. Cyclic tetraoximes have been synthesized by condensation of 1,3-propanediamine [19] with dichloroglyoxime, while polymeric complexes with the cyclic tetraoxime ligand have been obtained by interaction of *o*-phenylenediamine with nickel(II) salts in the first step and with dichloroglyoxime in the second step [21]. Tetraoxime molecules, especially the cyclic ones [19, 20, 22], could be widely used in the synthesis of binuclear coordination compounds, including those with polymeric structure.

The aim of this work was to synthesize the known tetraoxime [2] by condensing dichloroglyoxime with *m*-phenylenediamine (*m*PDA) and to obtain it in the form of single crystals, as its crystal structure had not been determined. As a result, different solvatomorphs of tetraoxime were obtained, two of which are polymorphs. Their chemical composition and structure were studied using modern spectral methods, while the structure of these compounds was studied by X-ray diffraction. All compounds were evaluated for biological activity against seven strains of non-pathogenic and phytopathogenic bacteria and fungi.

2. Materials and Methods

*Synthesis of bis(m-phenylenediamine)tetraoxime $H_4L{\cdot}2DMF$ (**1**).*

A mixture of 1,3-phenylenediamine (0.2 g, 0.2 mmol) and dichloroglyoxime (0.31 g, 0.2 mmol) in EtOH (10 mL) formed an orange-coloured solution which was stirred for 10 minutes at room temperature. Then Na_2CO_3 (0.12 g, 0.2 mmol) and H_2O (1.5 mL) were added, resulting in the formation of a brown-reddish precipitate. To completely dissolve the Na_2CO_3, the reaction mixture was heated at 45–50°C for 30–40 minutes, then stirred without heating for another 2 hours, by which time the reddish-yellow precipitate formed and was separated by filtration. The filtrate was allowed to crystallize at room temperature. The precipitate was washed sequentially with EtOH (3×2 mL) and Et_2O (3×2 mL), and

air-dried. After washing and drying, the compound **1** (0.12 g, 60%) was beige in colour. It is soluble in MeOH, DMF and DMSO, and insoluble in H_2O, EtOH, MeCN, and Et_2O. The colourless prismatic crystals of compound **1**, obtained from the filtrate after 4 days of crystallization, were further subjected to X-ray diffraction. M.p. 239–241°C.

Anal. Calcd. for $C_{11}H_{15}N_5O_3$: Calcd., %: C 49.80; H 5.70; N 26.42. Found, %: C 50.07; H 5.58; N 26.31.

IR spectra (cm^{-1}): 3200 (s), 3100 (w), 2972 (s), 2902 (m), 1647 (w), 1602 (vs), 1596 (vs), 1522 (w), 1496 (m), 1448 (w), 1353 (w), 1313 (m), 1289 (m), 1240 (m), 1189 (m), 1161 (w), 1080 (m), 1045 (s), 1017 (vw), 999 (vw), 958 (s), 938 (vs), 899 (s), 882 (m), 856 (w), 820 (w), 780 (m), 727 (w), 690 (s), 640 (s), 550 (vw), 488 (w), 447 (w), 420 (vw). (Intensities are given as: vs – very strong, s – strong, m – medium, w – weak, vw – very weak.)

^{1}H NMR (400.13 MHz, DMSO-d_6, ppm): δ 10.36 (br.s., 4H, >N–OH), 7.94 (s, 1H, H–C), 7.65 (br.s., 4H, NH), 6.85 (br.s., 2H, C_2–H), 6.37 (br.s., 6H, $C_{4,5,6}$–H), 2.88 and 2.73 (both s, 6H, –N(CH_3)$_2$).

^{13}C NMR (100.61 MHz, DMSO-d_6, ppm): δ 162.86 (>C=O), 152.0 (C_7, C_8), 144.7 (C_1), 140.0 (C_3), 128.2 (C_2), 112.0 ($C_{4,6}$), 109.8 (C_5), 36.28 and 31.29 (–N(CH_3)$_2$).

^{15}N NMR (40.54 MHz, DMSO-d_6, ppm): δ 29.5, 184.1.

Subsequent attempts to synthesize the coordination complexes of Zn(II), Mn(II), and Gd(III) with this ligand yielded cubic crystals that were subjected to X-ray diffraction. The analysis showed that the crystals consist solely of tetraoxime molecules with the following compositions: $H_4L{\cdot}2DMF$ (**2**), $H_4L{\cdot}3H_2O$ (**3**), and $H_4L{\cdot}2EtOH{\cdot}0.33H_2O$ (**4**).

Elemental analysis of the complexes for C, H, and N was performed using a Vario EL (III) Elemental Analyzer, and the metal content was determined using an AAS-1N atomic absorption spectrometer (Carl Zeiss).

Infrared spectra (IR) were recorded on a FT-IR Spectrum-100 Perkin Elmer spectrometer using ATR technique, in the range 650–4000 cm^{-1}.

^{1}H, ^{13}C and ^{15}N NMR spectra were recorded in DMSO-d_6 (99.95%) on a Bruker Avance DRX 400 spectrometer (400.13, 100.61, and 40.54 MHz). Chemical shifts (δ) are reported in ppm relative to the residual non-deuterated solvent peak (2.50 ppm for ^{1}H, 39.50 ppm for ^{13}C, and 45.00 ppm for ^{15}N). Coupling constants (J) are reported in Hertz (Hz). The following abbreviations were used to explain the multiplicities: s = singlet, d = doublet, t = triplet, q = quartet, qvin. = quintet, sex = sextet, m = multiplet, br.s = broad singlet. All reagents were purchased from commercial suppliers and used without further purification unless otherwise stated.

X-ray diffraction. The X-ray diffraction data of **1–4** crystals were collected with an Xcalibur E CCD diffractometer equipped with a CCD area detector and a graphite monochromator, using M*oKα* radiation (λ = 0.71073 Å) at room temperature (293 K). Data collection and reduction, and unit cell determination were performed using CrysAlis PRO software. Structure solution and refinement were carried out with SHELXS97 and SHELXL2014 software packages [23, 24]. Non-hydrogen atoms were refined anisotropically (full-matrix least squares on F^2). Hydrogen atoms were placed in calculated positions and refined using a riding model with U_{iso}(H) = 1.2U_{eq}(C). Hydrogen atoms bonded to oxygen were located from difference Fourier maps at an intermediate stage of refinement.

The crystallographic data have been deposited at the Cambridge Crystallographic Data Centre (CCDC) under deposit numbers 2352898–2352901 for compounds **1–4**, respectively. Copies of this information can be obtained free of charge from the CCDC, 12 Union Road, Cambridge CB2 1EZ, UK (Fax: +44 1223 336033; e-mail: deposit@ccdc.cam.ac.uk or via www.ccdc.cam.ac.uk).

Biological methods. The antimicrobial activity assessment of both compounds was evaluated against the following microorganisms: non-pathogenic Gram-positive and Gram-negative bacterial strains *Bacillus subtilis* NCNM BB-01 (ATCC 33608) and *Pseudomonas fluorescens* NCNM PFB-01 (ATCC 25323); phytopathogenic bacterial strains *Xanthomonas campestris* NCNM BX-01 (ATCC 53196), *Erwinia amylovora* NCNM BE-01 (ATCC 29780), and *Erwinia carotovora* NCNM BE-03 (ATCC 15713); as well as non-pathogenic yeast strains *Candida utilis* NCNM Y-22 (ATCC 44638) and *Saccharomyces cerevisiae* NCNM Y-20 (ATCC 4117).

Two-fold serial dilution method as described in [25] was used for the tests. First, 1 mL of peptone broth for bacteria and Sabouraud broth for yeast fungi was added to a series of 10 tubes each. Then 1 mL of the compound to be analyzed was added to the first test tube. The resulting mixture was pipetted and 1 mL of it was transferred to the next tube. The procedure was repeated up to tube no. 10 of the series. In this way, the concentration of the initial compound decreased two-fold in each subsequent tube. At the same time, test microbial cultures were prepared after growing for 24 hours. Subsequently, the tubes with titrated compound and the inoculum of test-microorganisms were kept in the thermostat at 35 °C for 24 hours. On the second day, a preliminary analysis of the results was made. The last tube from the series with no visible growth of the microorganisms detected is considered to be the minimum inhibitory concentration (MIC) of the compound. To estimate the minimum bactericidal and fungicidal concentrations, the contents of the test tubes with MIC and with higher concentrations were inoculated on peptone and

Sabouraud agar in Petri dishes using a bacteriological loop. The inoculated dishes were kept in thermostat at 35 °C for 24 hours. The concentration of the compound that inhibits the growth of any colony of microorganisms is considered to be the minimum bactericidal and fungicidal concentrations of the compound.

3. Results and Discussions

The synthesis of the target compound was achieved according to Figure 1 via interaction of dichloroglyoxime ($DClH_2$) with *m*-phenylenediamine in a 1:1 molar ratio in EtOH and DMF. The yield of compound **1** was 60%. Its structure was confirmed by spectral FTIR and ^{1}H, ^{13}C and ^{15}N NMR analysis, and single crystal X-ray diffraction. A new polymorph (**2**) of compound **1** was obtained in the presence of Zn(II) ions under similar conditions, and two new solvatomorphs were obtained in the presence of Mn(II) or Gd(III) ions. Their structures were confirmed by X-ray diffraction.

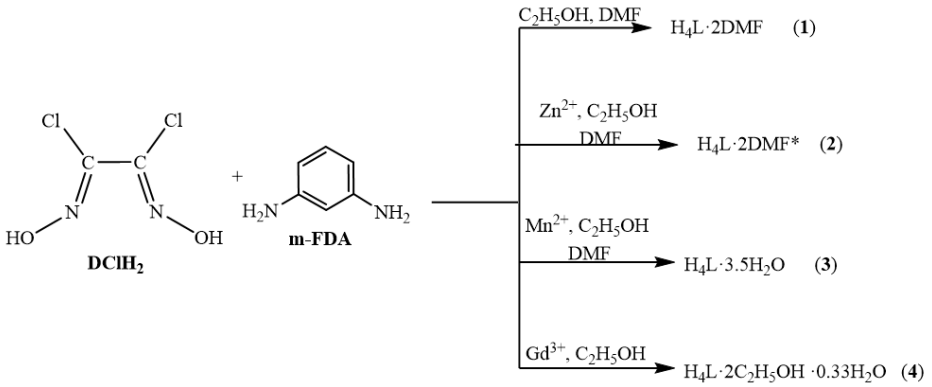

*The organic molecules have the same structure as **1**.

Figure 1. Synthesis of compounds **1–4**.

A very broad band of high intensity is observed in the IR spectrum of compound **1** at 3500–3000 cm^{-1}, which is mostly attributed to ν(OH) oscillations of oxime origin. The shoulder at 3100 cm^{-1} located on the long-wavelength side of the ν(OH) band is attributed to $\nu(CH)_{arom.}$ oscillations, and the absorption bands at 2972 and 2902 cm^{-1} to ν_{as}(CH) and ν_{s}(CH) of the CH_3 groups [26]. The absorption band of weak intensity at 1647 cm^{-1} can be attributed to ν(C=N) oscillations [27].

A composite band of the highest intensity is observed at 1620–1500 cm^{-1} spectral region with a more intense peak at 1602 cm^{-1} and another one at 1596 cm^{-1}. The first peak can be attributed to ν(C=O) oscillations in DMF, and the essential shift of this band to lower

wavelengths can be explained by the participation of the C=O group in the formation of relatively strong hydrogen bonds in the crystal lattice with the O$\cdots$H–O–2.748 Å oxime group. The second peak at 1596 cm^{-1} is attributed to δ(NH) frequencies (amide II, δ(NH)+ν(CN)) [28, 29], and the band at 1289 cm^{-1} to amide(III) vibrations [28, 29].

Absorption bands at 1496 and 1448 cm^{-1} are attributed to $\nu(C{=}C)_{arom.}$, and the band at 1313 cm^{-1} to ν(C–N) oscillations [28]. The very high intensity band at 938 cm^{-1} is attributed to the oscillations of the N–O oxime bond [27]. $\delta(CH)_{arom.pl}$ and especially $\delta(CH)_{arom.nonpl}$ absorption bands are well observed in the spectrum of compound **1**. The former appeared at 1161, 1080, and 1045 cm^{-1} for the 1,3-substituted aromatic rings, and the nonplanar ones for an isolated hydrogen atom and for three adjacent hydrogen atoms are attributed to the bands at 899 and 780 cm^{-1}, respectively. According to [26], the high intensity band at 690 cm^{-1} can be attributed to non-planar oscillations in 1,3-substituted aromatic compounds.

The ^{1}H, ^{13}C, and ^{15}N NMR analysis fully confirmed the structure of compound **1**. Thus, in the proton spectrum, broad singlets are observed at 6.85 ppm, belonging to protons from four secondary amine groups. Those from 7.65 ppm and 6.37 ppm are attributed to the unsubstituted C_2–H and C_4–H, C_5–H and C_6–H from aromatic rings of ligand **1**. The protons from four oxime groups appear at 10.92 ppm as broad singlets. The presence of a co-crystallized molecule of DMF is confirmed by three singlets at 7.94, 2.88, and 2.73 ppm, respectively.

The signals of tertiary carbon atoms (C_2, $C_{4,6}$, and C_5) from aromatic rings were registered at 128.23, 112.0 and 109.8 ppm, hile the quaternary $C_{1,3}$ appeared at 144.67 and 140.0 ppm. The signals of carbon atoms ($C_{7,8}$) from oxime groups is localized at 152.0 ppm. The carbon spectral data are completed by signals from the carbonyl group of the DMF molecule at 162.86 ppm and two amidic methyl groups at 36.28 and 31.29 ppm, respectively. Nitrogen atoms are represented by signals at 29.5 and 184.1 ppm in the ^{15}N NMR spectra.

The X-ray study showed that compounds **1** and **2** are two polymorphic forms, their formula is $H_4L{\cdot}2DMF$, and they crystallize in different space groups: **1** – in the centrosymmetric triclinic $P\bar{1}$ group, while **2** – in the monoclinic $P2_1/c$ group. Compounds **3** and **4** differ from **1** and **2** by solvate molecules. They crystallize in trigonal space groups $R\bar{3}$ and $R\bar{3}c$ with formulas $H_4L{\cdot}3H_2O$ and $H_4L{\cdot}2EtOH{\cdot}0.33H_2O$, respectively, being different solvatomorphs (Table 1). The molecular structure of these compounds allows the formation of a similar centrosymmetric organic macrocyclic compound via condensation of two molecules of *m*-phenylenediamine (*m*-FDA) with two molecules of dichloroglyoxime ($DClH_2$), in which the basic fragments alternate (Figure 2). In the oxime

groups of compounds **1–4**, the N–C, N–O and C–C bond lengths are within the ranges 1.283(4) – 1.291(3) Å, 1.415(4) – 1.426(3) Å, and 1.474(4) – 1.495(2) Å, respectively, corresponding to those established for uncoordinated dioximes [2, 30, 31, 32].

Table 1. Crystal data and structure refinement for **1–4**.

Parameters	*Value*			
	(1)	**(2)**	**(3)**	**(4)**
Formula	$C_{22}H_{30}N_{10}O_6$	$C_{22}H_{30}N_{10}O_6$	$C_{16}H_{23}N_8O_{7.5}$	$C_{20}H_{28.67}N_8O_{6.33}$
M_r / g mol^{-1}	530.56	530.56	447.42	482.51
cryst. system	triclinic	monoclinic	trigonal	trigonal
space group	$P\bar{1}$	$P2_1/c$	$R\bar{3}$	$R\bar{3}c$
a / Å	6.9940(5)	10.8055(9)	17.7522(10)	15.1147(10)
b / Å	8.7940(8)	9.9327(7)	17.7522(10)	15.1147(10)
c / Å	11.9818(8)	12.1433(8)	17.4127(10)	56.680(5)
α / °	101.291(7)	90	90	90
β / °	99.668(6)	95.955(7)	90	90
γ / °	111.270(8)	90	120	120
V, Å^3	650.02(10)	1296.25(17)	4752.3(6)	11214.1(18)
Z	2	4	18	18
D_{calc} / mg m^{-3}	1.355	1.359	1.407	1.286
μ / mm^{-1}	0.102	0.102	0.113	0.098
$F(000)$	280	560	2115	4596
crystal size / mm^3	0.55×0.30×0.08	0.40×0.40×0.03	0.38×0.35×0.30	0.20×0.15×0.01
Reflections collected/ independent reflections	4083/2407 (R_{int} = 0.0183)	4763/2399 (R_{int} = 0.0415)	3039/1968 (R_{int} = 0.0346)	6519/2215 (R_{int} = 0.0824)
Completeness to θ / %	99.7 (θ = 25.24)	99.8 (θ = 25.24)	99.7 (θ = 25.24)	99.8 (θ = 25.04)
Parameters	176	175	145	160
Goodness-of-fit on F^2	1.005	1.002	1.004	1.002
final R_1, wR_2	R_1 = 0.0446, wR_2 = 0.1276	R_1 = 0.0621, wR_2 = 0.1306	R_1 = 0.0677, wR_2 = 0.1408	R_1 = 0.0765, wR_2 = 0.1650
R indices (all data)	R_1 = 0.0565, wR_2 = 0.1365	R_1 = 0.1182, wR_2 = 0.1569	R_1 = 0.1250, wR_2 = 0.1688	R_1 = 0.1678, wR_2 = 0.2003
largest diff. peak and hole, eÅ^{-3}	0.271, –0.279	0.275, –0.332	0.243, –0.321	0.352, –0.338

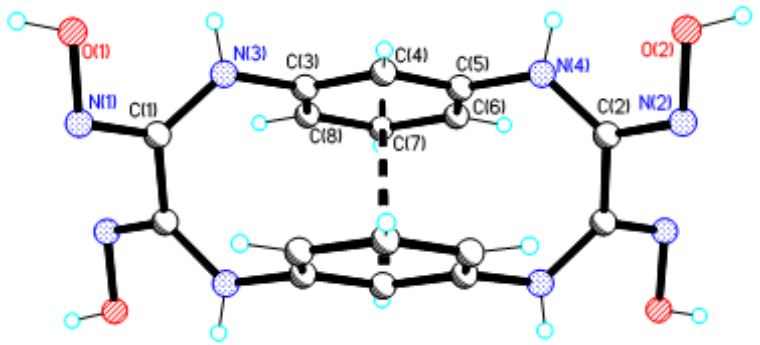

Figure 2. The molecular structure of the H_4L proligand of 1.

These organic molecules in the compounds are stabilized by $\pi \cdots \pi$ interactions, with distances between the aromatic centers ranging from 3.376 to 3.507 Å. Analysis of the CSD results [32] revealed a different arrangement of the dioxime moiety, varying from *cis*- to *trans*- forms. For example, in the organic compounds stabilized by rigid fragments such as cyclohexane, naphthoquinone, or quinoxaline [33, 34, 35, 36], the NCCN torsion angles are in the range of 2.07–20.08°, in compounds with more bulky substituents [30, 37] - in the range of 58.47–71.70°, and in compounds with -CH_3 or -CH_2-CH_3 as a substituent [38, 39, 40] - in the range of 179.37–180.0°. For compounds **1–4**, the values of the NCCN torsion angles in the dioxime fragments are equal to 59.8°, 67.7°, 66.5°, and 53.9°, respectively, so we can assume that they are quite rigid.

In the crystal of compound **1**, the H_4L organic molecules are linked by O(2)–H(2)$\cdots$N(2) intermolecular hydrogen bonds (Figure 3 (a), Table 2), forming centrosymmetric chains in which the $R_2^2(6)$ supramolecular heterosyntons are observed. These chains are joined in the crystal by DMF molecules of crystallization, which participate in the formation of N(4)–H(2N)$\cdots$O(3) and O(1)–H(1)$\cdots$O(3) intermolecular hydrogen bonds, as well as C–H$\cdots$O and C–H$\cdots$N fine hydrogen bonds.

In the crystal of compound **2**, the H_4L organic molecules form chains through O(2)–H(2)$\cdots$O(1) and N(4)–H(2N)$\cdots$N(1) intermolecular hydrogen bonds (Figure 3 (b), Table 2). These are stabilized by fine C–H$\cdots$N hydrogen bonds and linked to each other *via* C–H$\cdots$O interactions. DMF molecules of crystallization are attached to these chains via O(1)–H(1)$\cdots$O(3) intermolecular hydrogen bonds.

In the crystal of compound **3**, a complicated system of intermolecular hydrogen bonds was observed, in which three H_4L organic molecules are bonded around the three-fold inversion axis by O(1)–H(1)$\cdots$N(1), forming $R_3^3(6)$ supramolecular heterosyntons in the

form of equilateral triangles. The structure is developed by the second O(1)–H(1)···N(1) bond in the layer, stabilized by N(3)–H(1N) bonds. The 3D supramolecular structure is extended by a number of bonds involving water molecules and fine C–H···O hydrogen bonds.

Table 2. Hydrogen bond distances (Å) and angles (°) in **1–4**

D–H···A	d(H···A)	d(D···A)	∠(DHA)	Symmetry transformations for A
		1		
O(1)–H(1)···O(3)	1.98	2.746(2)	155	$-x+1,-y+1,-z$
O(2)–H(2)···N(2)	2.05	2.722(2)	139	$-x,-y,-z+1$
N(4)–H(2N)···O(3)	2.27	3.012(2)	145	x,y,z
C(4)–H(4)···O(1)	2.62	3.345(2)	135	$-x+1,-y+1,-z$
C(10)–H(10A)···N(2)	2.63	3.428(3)	141	$-x+1,-y,-z+1$
C(11)–H(11A)···O(2)	2.65	3.580(3)	163	$-x+1,-y+1,-z+1$
		2		
O(1)–H(1)···O(3)	1.82	2.636(3)	170	x,y,z
O(2)–H(2)···O(1)	2.04	2.826(3)	160	$-x+2,y+1/2,-z+3/2$
N(4)–H(2N)···N(1)	2.49	3.215(3)	143	$x,-y+1/2,z-1/2$
C(4)–H(4)···N(1)	2.58	3.270(4)	132	$x,-y+1/2,z-1/2$
C(6)–H(6)···O(2)	2.63	3.478(4)	152	$-x+2,y+1/2,-z+3/2$
		3		
O(1)–H(1)···N(1)	1.94	2.752(3)	170	$-x,x-y,z$
O(2)–H(2)···O(2W)	2.00	2.742(5)	156	$x-y+2/3,x+1/3,-z+1/3$
N(3)–H(1N)···O(2)	2.28	3.016(3)	144	$-x+2/3,x-y+1/3,z+1/3$
N(4)–H(2N)···O(1W)	2.03	2.854(4)	160	$-x+y+1/3,-x+2/3,z-1/3$
C(4)–H(4)···O(2W)	2.56	3.484(6)	175	$-x+1/3,-y+2/3,-z+2/3$
C(10W)–H(1W)···N(2)	1.95	2.952(6)	156	$-x+y+1/3,-x+2/3,z+2/3$
O(1W)–H(2)···O(1)	2.11	2.824(3)	140	x,y,z
O(2W)–H(1)···O(1W)	1.91	1.752(5)	160	x,y,z
O(2W)–H(2)···O(1W)	2.32	3.180(6)	166	$x-y,x,-z+1$
		4		
O(1)–H(1)···O(1)	1.93	2.686(3)	152	$x-y,x,-z$
O(2)–H(2)···O(3)	1.86	2.655(5)	165	x,y,z
N(3)–H(1N)···N(1)	2.10	2.923(5)	161	$y,-x+y,-z$
O(3)–H(3)···N(2)	2.11	3.012(5)	164	$x-y+2/3,-y+4/3,-z-1/6$
C(10)–H(10)···O(1)	2.55	3.469(10)	158	$y+2/3,x+1/3,-z-1/6$

The H_4L molecule in **4** is located on the crystallographic inversion center and thus has C_i molecular symmetry. The molecules connected in the crystal by a three-fold inversion axis are linked by O(1)–H(1)$\cdots$O(1) hydrogen bonds involving the glyoxime groups in supramolecular $R^6{}_6(12)$ heterosyntons in the form of regular hexagons. Each of the molecules is involved in the formation of two such hexagons, resulting in a supramolecular layer parallel to the (ab) plane (Figure 3 (d), Table 2).

The crystallization water molecules, which do not form hydrogen bonds with the basic components, are located in these hexagonal channels. This molecular arrangement is also stabilized via N(3)–H(1N)$\cdots$N(1) hydrogen bonds and, as a result, there are observed $R^2{}_2(8)$ graph sets formed by these two hydrogen bonds are observed in the structure.

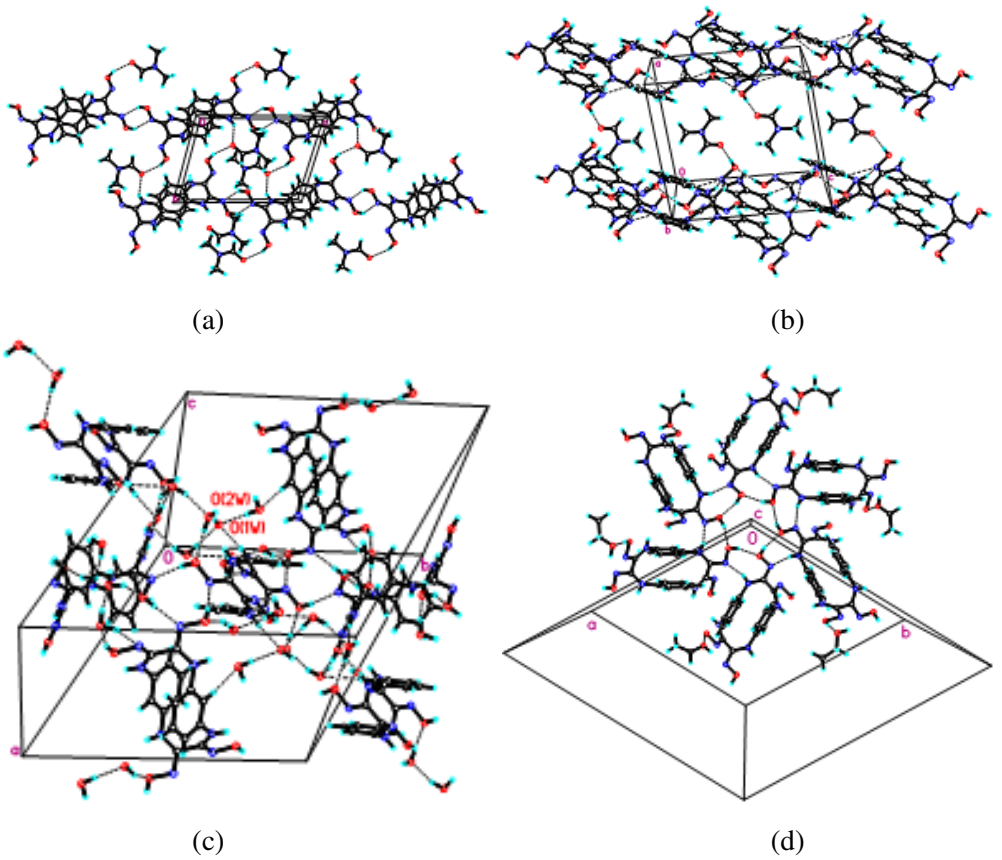

Figure 3. The packing mode of the components in the crystal of compounds **1–4** (a-d)

The other two hydroxyl groups of the glyoxime fragments are involved in hydrogen bonds as proton donors with ethanol molecules via intermolecular O(2)–H(2)$\cdots$O(3) hydrogen bonds. As these solvent molecules form O(3)–H$\cdots$N(2) and C(10)–H$\cdots$O(1)

hydrogen bonds with atoms in neighboring layers, 3D supramolecular systems are formed in the crystal.

A detailed literature search in the field of biological activity of *vic*-dioximes yielded some relevant bibliographic references. In one of them, the authors report that the *vic*-dioxime ligand bearing one naphthyl disodium disulfonate moiety has no inhibitory effect on the growth of *Rhodotorula rubra*, *Kluyveromyces marxianus*, *Aspergillus fumigatus* and *Mucor pusillus* fungal strains compared to its metal Cu^{II}, Ni^{II}, Zn^{II}, Cd^{II} complexes [41].

Another research group conducted *in vitro* assessments of some 3- and 4-substituted benzaldehyde hydrazones *vic*-ligands and their Cu^{II}, Ni^{II}, Co^{II} complexes on 18 strains of bacteria and yeasts [42]. The authors mentioned that all tested compounds exhibit moderate antimicrobial activity, the ligands being generally more active. In this sense, the mono-3-methylbenzaldehyde hydrazone *vic*-dioxime and mono-4-methoxybenzaldehyde hydrazone *vic*-dioxime must be mentioned. These ligands have shown slightly higher activities against *Bacillus thrungiensis* and strong activity against *Candida utilis*, *C. albicans*, *C. glabrata*, *C. tropicalis*, and *Saccharomyces cerevisiae*, compared to the reference compounds.

Authors [43] performed a comparative study of the antibacterial activity of two *vic*-dioxime ligands containing one *p*-tolyl and benzyl-piperazinyl, and *bis*-benzyl-piperazinyl radicals and their Ni^{II}, Cu^{II}, Co^{II}, Zn^{II} metal complexes. The study demonstrates that only *bis*-benzyl-piperazinyl-containing ligands show weak antibacterial activity.

In vitro inhibition activity of the tetraoxime proligand **1** was assessed against both non-pathogenic Gram-positive and Gram-negative bacteria (*Bacillus subtilis* and *Pseudomonas fluorescens*), phytopathogenic (*Xanthomonas campestris*, *Erwinia amylovora*, *E. carotovora*) bacteria, and yeast-fungi (*Candida utilis* and *Saccharomyces cerevisiae*) (Table 3).

Table 3. *In vitro* antifungal and antibacterial activities of **1**

Comp.	MBC and MFC, %						
	B. subtilis	*P. fluorescens*	*E. amylovora*	*E. carotovora*	*X. campestris*	*C. utilis*	*S. cerevisiae*
mFD	n/a	n/a	n/a	n/a	n/a	n/a	n/a
1	0.015	0.03	0.015	0.03	0.015	0.015	0.015
Control	0.06	0.06	0.06	0.06	0.03	0.06	0.03

Control – Augmentin solutin, MBC – minimum bactericidal concentration,
MFC – minimum fungicidal concentration, n/a – non active.

Compound **1** exhibits average antibacterial and antifungal properties in the concentration range of 2 – 4% for bacteria and 4% for fungi.

4. Conclusions

The condensation of dichloroglyoxime with *m*-phenylenediamine leads to the formation of a cyclic tetraoxime, as the -NH_2 groups in the two fragments of *m*-phenylenediamine are positioned in the exo-position. The newly obtained tetraoxime was tested for antimicrobial activity. The obtained results showed that compound **1** exhibited moderate antibacterial and antifungal properties in the concentration range of 2–4% for bacteria and 4% for fungi. In the presence of Zn(II) ions under similar conditions, only one new polymorph of compound **1** – $H_4L{\cdot}2DMF$ (**2**) – was obtained, while in the presence of Mn(II) or Gd(III) ions, two new solvatomorphs were formed – $H_4L{\cdot}3.5H_2O$ (**3**) and $H_4L{\cdot}2C_2H_5OH{\cdot}0.33H_2O$ (**4**). It is likely that the rigid glyoxime fragments in this molecule prevent coordination with the transition metal ions.

Acknowledgements

This work was supported by subprograms 010602, 011202 and 010601. Authors are grateful to the National Collection of Non-Pathogenic Microorganisms (NCNM) of the Institute of Microbiology and Biotechnology of Moldova Technical University for offering the microbial cultures for antimicrobial testing.

References

[1] KANNO, H., YAMAMOTO, H. *European patent*, 0,636,605A1, 1994.

[2] KAKANEJADIFARD, A., SHARIFI, A., DELFANI, F., RANJBAR, B., NADERIMANESH, H. Synthesis of di and tetraoximes from the reaction of phenylendiamines with dichloroglyoxime. *Iranian Journal of Chemistry and Chemical Engineering*, 2007, vol. 26, no. 4, pp. 63–67. DOI: https://doi.org/10.30492/IJCCE.2007.7602

[3] BOYER, J.H. Increasing the index of covalent oxygen bonding at nitrogen attached to carbon. *Chemical Reviews*, 1980, vol. 80, no. 6, pp. 495–561. DOI: https://doi.org/10.1021/cr60328a002

[4] SCHRAUZER, G.N., KOHNLE, J. Coenzyme B12 – modelle. *Chemische Berichte*, 1989, vol. 97, no. 11, pp. 3056–3064. DOI: https://doi.org/10.1002/cber.19640971114 (in German)

[5] SERIN, S. New vic-dioxime transition metal complexes. *Transition Metal Chemistry*, 2001, 26(3), pp. 300–306. DOI: https://doi.org/10.1023/A:1007163418687

[6] BALSAMO, A., MACCIHA, B., MARTINELLI, A., ORLANDINI, E., ROSELLO, A., MACCHIA, F., BROCALLI, G., DOMIANO, P. Synthesis and antimicrobial properties of substituted 3-aminoxy-(E)-2-methoxyiminopropionyl penicillins and cephalosporins. *European Journal of Medicinal Chemistry*, 1990, vol. 25, no. 3, pp. 227–233. DOI: https://doi.org/10.1016/0223-5234(90)90205-H

[7] ÖZTÜRK, A., BABAHAN, İ., SARIKAVAKLI, N., HÖKELEK, T. (E, E)-1-(2-Hydroxyimino-1-phenylethylidene) semicarbazide monohydrate. *Acta Crystallographica, Section E – Crystallographic*

Communications, 2009, vol. 65, no. 5, pp. o1059–o1060. DOI: https://doi.org/10.1107/S1600536809013865

[8] BABAHAN, İ., ANIL, H., SARIKAVAKLI, N. Synthesis of novel tetraoxime derivative with hydrazone side groups and its metal complexes. *Turkish Journal of Chemistry*, 2011, vol. 35, no. 4, pp. 613–624. DOI: https://doi.org/10.3906/kim-1003-105

[9] KANDAZ, M., YILMAZ, İ., KESKIN, S., KOCA, A. Synthesis, spectroscopy and redox properties of a novel (E-E) vic-dioxime and its mono-, di- and trinuclear complexes bearing an 18-membered N2O2S2 macrocycle. *Polyhedron*, 2002, vol. 21, no. 8, pp. 825–834. DOI: https://doi.org/10.1016/S0277-5387(02)00860-4

[10] MELSON, G.A. *Coordination chemistry of macrocyclic compounds*. New York, USA. Plenum Press, 1979.

[11] DILWORTH, J.R., PARROTT, S.J. The biomedical chemistry of technetium and rhenium. *Chemical Society Reviews*, 1998, vol. 27, no. 1, pp. 43–55. DOI: https://doi.org/10.1039/A827043Z

[12] BLOWER, P.J. Small coordination complexes as radiopharmaceuticals for cancer targeting. *Transition Metal Chemistry*, 1997, vol. 23, no. 1, pp. 109–112. DOI: https://doi.org/10.1023/A:1006926505754

[13] WOLKERT, W.A., HOFFMAN, T.J. Therapeutic radiopharmaceuticals. *Chemical Reviews*, 1999, vol. 99, no. 9, pp. 2269–2292. DOI: https://doi.org/10.1021/cr.9804386

[14] OHTA, K., HIGASHI, R., IKEJIMA, M., YAMAMOTO, I., KOBAYASHI, N. Disk-like liquid crystals of transition metal complexes. Part 21 – Critical molecular structure change from columnar to lamellar liquid crystal in bis(diphenylglyoximato)nickel(II)-based complexes. *Journal of Materials Chemistry*, 1998, vol. 9, no. 8, pp. 1979–1991. DOI: https://doi.org/10.1039/A800897C

[15] MALMSTROEM, B.G. Vectorial chemistry in bioenergetics: cytochrome c oxidase as a redox-linked proton pump. *Accounts of Chemical Research*, 1993, vol. 26, no. 6, pp. 332–338. DOI: https://doi.org/10.1021/ar00030a006

[16] LARANLEIRA, M.C.M., MARUSAK, R.A., LAPPIN, A.G. Driving force effects in proton-coupled electron transfer. *Inorganica Chimica Acta*, 2000, vol. 300–302, pp. 186-190. DOI: https://doi.org/10.1016/S0020-1693(99)00558-7

[17] BAKIR, M. Electrochemical properties of the first Re(I)-carbonyl compound of di-2-pyridyl ketoneoxime (dpk.oxime), fac-Re(CO)3(dpk.oxime)Cl, in non-aqueous media. *Journal of Electroanalytical Chemistry*, 1999, vol. 466, no. 1, pp. 60–66. DOI: https://doi.org/10.1016/S0022-0728(99)00122-9

[18] BAKIR, M.- MCKENZIE, J.A.M. Rhenium(I) di- and tri-carbonyl compounds of polypyridyl-like ligands: electrochemical reactions of fac-[Re(CO)3(dpk)Cl] (dpk = di-2-pyridylketone) with electrophiles and Group I and II metal ions. *Journal of the Chemical Society, Dalton Transactions*, 1997, vol. 19, pp. 3571–3578. DOI: https://doi.org/10.1039/A608470B

[19] KURTOĞLU, M., İSPİR, E., KURTOĞLU, N., TOROĞLU, S., SERİN, S. New soluble coordination chain polymers of nickel(II) and copper(II) ions and their biological activity. *Transition Metal Chemistry*, 2005, vol. 30, no. 6, pp. 765–770. DOI: https://doi.org/10.1007/s11243-0056273-7

[20] KAKANEJADIFARD, A., KHAJEHKOLAKI, A., RANJBAR, B., MANESH-NADERI, H. Synthesis of new dioximes and tetraoximes from reaction of aminothiophenoles with dichloroglyoxime. *Asian Journal of Chemistry*, 2008, vol. 20, no. 4, pp. 2937–2946.

[21] KURTOĞLU, M., SERİN, S. Template synthesis of two new glyoxime derivatives. Characterization and investigation of their complexes with Ni(II), Cu(II) and Co(II) metal ions. *Synthesis and Reactivity in Inorganic and Metal-Organic Chemistry*, 2001, vol. 31, no. 7, pp. 1129–1139. DOI: https://doi.org/10.1081/SIM-100106853

[22] COBURN, M.D. Picrylamino-substituted heterocycles. II. Furazans. *Journal of Heterocyclic Chemistry*, 1968, vol. 5, no. 1, pp. 83–87. DOI: https://10.1002/jhet.5570050114

[23] SHELDRICK, G.M. A short history of SHELX. *Acta Crystallographica, Section A*, 2008, A64 (1), pp. 112–122. DOI: https://doi.org/10.1107/S0108767307043930

[24] SHELDRICK, G.M. Crystal structure refinement with SHELXL. *Acta Crystallographica Section C*, 2015, C71 (1), pp. 3–8. DOI: https://doi.org/10.1107/S2053229614024218

[25] CIOCARLAN, A., DRAGALIN, I., ARICU, A., LUPASCU, L., CIOCARLAN, N., POPESCU, V. Chemical composition and antimicrobial activity of the Levisticum officinale W.D.J. Koch essential oil. *Chemistry Journal of Moldova*, 2018, vol. 13, no. 2, pp. 63–68. DOI: https://doi.org/10.19261/cjm.2018.514

[26] NAKANISHI, K. *Infrared absorption spectroscopy*. Tokyo, Japan. Holden Day, 1962.

[27] GORDON, A., FORD, R. *The Chemist's Companion: A Handbook of Practical Data, Techniques, and References*, New York: Wiley, 1972.

[28] BELLAMY, L.J. *Infrared spectra of complex molecules*. New York, USA. Wiley, 1954.

[29] TARASEVICH, B.N. *IR Spectra of the Main Classes of Organic Compounds*, Moscow, 2012.

[30] URECHE, D., BULHAC, I., CIOCARLAN, A., ROSHCA, D., et al. Novel vic-dioximes: synthesis, structure characterization and antimicrobial activity evaluation. *Turkish Journal of Chemistry*, 2021, vol. 45, no. 6, pp. 1873–1881. DOI: https://doi.org/10.3906/kim-2104-24

[31] BOUROSH, P.N., COROPCEANU, E.B., RIJA, A.P., URECHE, D., CILOCI, A.A., CLAPCO, S.F., DVORNINA, E.G., LABLIUC, S.V., BULHAC, I.I. Synthesis and structures of disulfanileamideglyoxime and Ni(II) and Cu(II) complexes with this ligand stimulating the proteolytic properties of [Cu(DsamH2)3]SO4·5H2O. *Russian Journal of Coordination Chemistry*, 2022, vol. 48, no. 1, pp. 41–51. DOI: https://doi.org/10.1134/S1070328422010018

[32] KAKANEJADIFARD, A., AMANI, V. (2Z, 3Z)-3,4-Dihydro-2H-1,4-benzothiazine-2,3-dione dioxime dihydrate. *Acta Crystallographica, Section E – Crystallographic Communications*, 2008, vol. 64, no. 8, pp. o1628. DOI: https://doi.org/10.1107/S1600536808023301

[33] ALLEN, F.H. The Cambridge Structural Database: a quarter of a million crystal structures and rising. *Acta Crystallographica, Section B – Structural Science, Crystal Engineering and Materials*, 2002, vol. 58, no. 3, pp. 380–388. DOI: https://doi.org/10.1107/S0108768102003890

[34] NÄSÄKKÄLÄ, M., SAARINEN, H., KORVENRANTA, J., NÄSÄKKÄLÄ, E. The crystal structure of (1Z, 2E)-1,2-naphthoquinone dioxime. *Acta Chemica Scandinavica*, 1977, 31A, pp. 469–472. DOI: https://doi.org/10.3891/acta.chem.scand.31a-0469

[35] COROPCEANU, E.B., CROITOR, L., SIMINEL, A.V., CHUMAKOV, Yu., FONARI, M.S. The luminescence attenuation in the solid state by fluoride anion entrapped in the one-dimensional Zn(II) dioximate and mononuclear Cd(II) dioxime compounds. *Polyhedron*, 2016, vol. 109, pp. 107–114. DOI: https://doi.org/10.1016/j.poly.2016.01.043

[36] KAKANEJADIFARD, A., AMANI, V. (2Z, 3Z)-Quinoxaline-2,3(1H,4H)-dione dioxime. *Acta Crystallographica, Section E – Crystallographic Communications*, 2008, vol. 64, no. 8, p. o1512. DOI: https://doi.org/10.1107/S1600536808021570

[37] STENKAMP, R.E., JENSEN, L.H., MURPHY, T.B., ROSE, N.J. Structure of a benzene solvate of α-furildioxime. *Acta Crystallographica, Section B – Structural Science, Crystal Engineering and Materials*, 1982, vol. 38, no. 4, pp. 1169–1172. DOI: https://doi.org/10.1107/S0567740882005226

[38] BISWAS, S., SAHA, R., STEELE, I.M., KUMAR, S., DEY, K. Co-crystals of 2,3-dimethylquinoxaline (DMQ) and dimethylglyoxime (DMG) in 1:1 and 1:2 ratios and hirshfeld surface analysis. *Journal of Chemical Crystallography*, 2013, vol. 43, no. 9, pp. 493–501. DOI: https://doi.org/10.1007/S10870-013-0449-3

[39] HAMILTON, W.C. A neutron diffraction refinement of the crystal structure of dimethylglyoxime. *Acta Crystallographica*, 1961, vol. 14, no. 2, pp. 95–100. DOI: https://doi.org/10.1107/S0365110X61000450

[40] BEIRAKHOV, A.G., ORLOVA, I.M., ROTOV, A.V., IL'IN, E.G., et al. Conformation of diethylglyoxime in uranyl complexes. *Russian Journal of Inorganic Chemistry*, 2016, vol. 61, no. 11, pp. 1522–1529. DOI: https://doi.org/10.1134/S0036023616120032

[41] KURTOĞLU, M., İSPİR, E., KURTOĞLU, N., SERİN, S. Novel vic-dioximes: Synthesis, complexation with transition metal ions, spectral studies and biological activity. *Dyes and Pigments*, 2008, vol. 77, no. 1, pp. 75–80. DOI: https://doi.org/10.1016/j.dyepig.2007.03.010

[42] BABAHAN, I., POYRAZOĞLU ÇOBAN, E., ÖZMEN, A., BIYIK, H., ISMAN, B. Synthesis, characterization and biological activity of vic-dioxime derivatives containing benzaldehydehydrazone groups and their metal complexes. *African Journal of Microbiology Research*, 2011, vol. 5, no. 3, pp. 271–283.

[43] BILGE, T., UĞUR, A. Preparation and spectral and biological investigation of vic-dioxime ligands containing piperazine moiety and their mononuclear transition-metal complexes. *Synthetic Communications*, 2013, vol. 43, no. 24, pp. 3307–3314. DOI: https://doi.org/10.1080/00397911.2013.777743

Received: March 18, 2025 *Accepted: July 02, 2025*

(Dumitru Ureche, Ion Bulhac, Alexandru Ciocarlan, Lucian Lupascu) Institute of Chemistry, Moldova State University
E-mail address: d.ureche@yahoo.com, ionbulhac@yahoo.com, algciocarlan@yahoo.com, lucianlupascu75@gmail.com

(Pavlina Bourosh) Institute of Applied Physics, Moldova State University
E-mail address: bourosh.xray@gmail.com